Beeporter: tools for high-throughput analyses of pollinator-virus infections

Jay D. Evans*, Olubukola Banmeke, Evan C. Palmer-Young, Yanping Chen, Eugene V. Ryabov*

USDA-ARS Agricultural Research Service, Bee Research Laboratory, 10300 Baltimore Avenue, Beltsville, MD 20705, USA

∗ Corresponding authors.

E-mail addresses: Jay.evans@usda.gov (https://orcid.org/0000-0002-0036-4651).

Olubukola.banmeke@usda.gov , (https://orcid.org/0000-0002-0010-5887)

Evan.palmer-young@usda.gov (https://orcid.org/0000-0002-9258-2073)

Judy.chen@usda.gov (https://orcid.org/0000-0002-5224-1100)

Eugene.ryabov@usda.gov, eugene.ryabov@gmail.com, (https://orcid.org/0000-0002-4265-9714).

Key words: Deformed wing virus, green fluorescent protein, nanoluciferase, insect immunity, pollination, RNA virus, host-pathogen interactions.

ABSTRACT

Pollinators are in decline thanks to the combined stresses of disease, pesticides, habitat loss, and climate. Honey bees face numerous pests and pathogens but arguably none are as devastating as Deformed wing virus (DWV). Understanding host-pathogen interactions and virulence of DWV in honey bees is slowed by the lack of cost-effective high-throughput screening methods for viral infection. Currently, analysis of virus infection in bees and their colonies is tedious, requiring a well-equipped molecular biology laboratory and the use of hazardous chemicals. Here we describe cDNA clones of DWV tagged with green fluorescent protein (GFP) or nanoluciferase (nLuc), providing high-throughput detection and quantification of virus infections. GFP fluorescence is recorded non-invasively in living bees via commonly available long-wave UV light sources and a smartphone camera or a standard ultraviolet transilluminator gel imaging system. Nonlethal monitoring with GFP allows high-throughput screening and serves as a direct breeding tool for identifying honey bee parents with increased antivirus resistance. Expression using the nLuc reporter strongly correlates with virus infection levels and is especially sensitive. Using multiple reporters, it is also possible to visualize competition, differential virulence, and host tissue targeting by co-occuring pathogens. Finally, it is possible to directly assess the risk of cross-species 'spillover' from honey bees to other pollinators and vice versa.

INTRODUCTION

Insects and other arthropods are prime vectors of disease agents, including a suite of viruses important for human, plant, and animal health. In addition, many insects play beneficial roles in nature and for humankind. Pollination by insects adds at least $20 billion annually to the U.S. agricultural economy (Chopra, Bakshi, & Khanna, 2015) and hundreds of billions of dollars worldwide (Gallai, Salles, Settele, & Vaissière, 2009). Honey bees are the preeminent agricultural pollinators, thanks to their numbers and the mobility of their colonies. Despite their critical roles in agriculture through pollination and hive products`, honey bee populations are under threat. Half of all honey bee colonies are lost and replaced annually in the U.S. (Steinhauer et al., 2018). Declines of unmanaged pollinators, from bumble bees to thousands of ground-nesting solitary bees, are also evident in nature (Rollin et al., 2020; Rosenberger & Conforti, 2020), and have been linked to the emergence of new infectious disease agents (Tehel, Streicher, Tragust, & Paxton, 2020).

Diseases are a major cause of honey bee losses, especially diseases that are driven by parasitic mites. While mites themselves impact bees, it is the viruses they carry, and Deformed wing virus (DWV) in particular, that drive colony mortality (Dainat, Evans, Chen, Gauthier, & Neumann, 2012; Grozinger & Flenniken, 2019). Nevertheless, no effective treatments are commercially available for honey bee viruses. Identification of new viral controls requires the screening of hundreds of candidate drugs, in line with similar efforts for human medicine and large-animal disease work. This high-throughput screening is best carried out with living bees since this allows the simultaneous identification of off-target effects of chemicals on bees themselves.

A number of cloned viruses expressing fluorescent reporters, mainly mammalian and plant, have been developed (Cheng et al., 2020; Mei, Liu, Zhang, Hill, & Whitham, 2019; Wang et al., 2020; Xie et al., 2020).These viruses have been used to assess virus replication in a range of cells, tissues, and organisms, greatly advancing our understanding of virus biology and virus-host interactions. Here we describe protocols for *in vivo* monitoring of viral growth in honey bees. The strength of this protocol is the pairing of infectious viral cDNA clones (Ryabov et al., 2019) with a gene encoding the reporters GFP (Ryabov et al., 2020) or nanoluciferase (nLuc). Bees infected by these clones provide a reliable visual signal that can be screened readily and quantitatively with a standard digital camera. By comparing fluorescent signals with quantitative-RT-PCR estimates of viral loads in the same bees, we see excellent correlations, indicating that GFP fluorescence by itself is a good surrogate for molecular quantification of viral load. Nanoluciferase (nLuc) is a newly developed small luciferase reporter enzyme with the brightest bioluminescence reported to date (Hall et al., 2012). The monitoring of DWV infection by observing (recording) GFP fluorescence in live pupae, or by testing the luminescent activity of nLuc, allows investigations of viral replication dynamics at the level of insects. In order to increase sensitivity and specificity, we also describe an assay reliant on fluorescence measurements using a plate-reading spectrophotometer. After optimizing each strategy, we present the methods used for validation and refinement of conditions.

Honey bee researchers can benefit from this system via virus assays that would normally involve flying bees or bees in cages, saving labor costs. The GFP reporter allow for immediate non-invasive screens of viral loads, and both reporter systems avoid expensive and time-consuming RNA extraction, reverse transcription and quantitative-PCR steps. Companies and researchers seeking new bee medicines will be able to study in-house or novel candidate drugs

against these viruses, speeding their searches and reducing the need for specialists in molecular biology (Tauber et al., 2019). Regulators devoted to testing the impacts of pesticides and other stressors on bee health could assess those impacts through virus loads via this method since viruses are a strong indicator of honey bee stress (Nazzi & Pennacchio, 2018).

Finally, honey bee queen breeding is a million-dollar industry. Bee breeders seeking viral resistance can benefit from a reliable and quick assay for viral resistance in different bee lineages. Breeders could incorporate this system in their selective breeding program, giving them an integrated estimate of virus resistance in their breeder lines, without molecular-genetic resources or skills. In fact, since one of the two protocols described below is non-lethal, individual queens and reproductive males in specific breeding programs might be screened during development as a direct assay for their own breeding value prior to mating. This latter trait has not previously been possible since current screening tools for honey bee viruses involve sacrificing bees for RNA extraction.

In summary, while genetic techniques are available for quantifying virus loads in pollinators, these techniques are time consuming, relatively expensive, lethal to subjects, and dependent on expensive fixed laboratory equipment. The described protocols are highly flexible in terms of host life stages or tissues and, given investment in the development of infectious clones, is applicable in all insect-virus systems. Understanding disease ecology is vital for understanding the stability and formation of ecosystems, and similarly important for mitigating the effects of disease on ecosystem services important for human health and well-being.

MATERIALS AND METHODS

Reagents and Biological Materials

- Strong honey bee source colonies maintained with low levels (below 1%) of the parasitic *Varroa destructor* mites that vector Deformed wing virus.
- Full-length DWV cDNA clones derived from virulent Maryland isolate pDWV-304 (GenBank accession number MG831200) with the sequences encoding enhanced green fluorescent protein (GFP), or nanoluciferase (nLuc) inserted in frame at the leader protein-viral protein 2 (LP-VP2) border of the DWV cDNA (Ryabov et al., 2020).
- HiScribe T7 High Yield RNA Synthesis Kit (New England Biolabs, Cat. No. E2050S)
- Nano-Glo Luciferase assay system (Promega, Cat. No. N1110)
- 0.22 μm nylon membrane syringe filter (Thermofisher)
- Disposable (100 mm) Petri dishes
- Whatman filter paper folded to separate injected pupae
- Phosphate buffered saline (PBS)
- Disposable 31G insulin syringes, with 6 mm needle, capacity 300 μL (BD Becton Dickison)

Optional materials, for assay validation, not required for protocol:

- Black, clear-bottom 96-well plates (Corning)
- For quantification of DWV loads in the honey bee by RT-qPCR: TRIzol reagent, RNeasy RNA extraction kit (optional), Superscript III Reverse transcriptase, random hexanucleotides, SYBR-Green mix (and DWV-GFP-specific qPCR primers as in (Ryabov et al., 2020) and nLuc-specific qPCR primers (5'-GAAGGCATCGCCGTGTTCGACG-3' and 5'-CGCCAGAATGCGTTCGCACAGC-3').

Equipment

- Incubator with manual (dish) system for humidity control
- Micro-syringe injection pump and a microprocessor-based controller, UMP3/Micro4 (WPI - World Precision Instruments).
- UV transillumination table with low-wavelength (395 nm) light source and/or handheld UV 'blacklight at 365 nm.
- Digital smartphone camera. Can also use gel-documentation system with attached camera (UVP, Bioimaging Systems)

Optional equipment, for assay validation, not required for protocol:

- Fluorescence-equipped plate reader capable of excitation at 480 nm and measurement of emission at 520 nm and at 460 nm SpectraMax Paradigm^{TM} Multi-mode detection platform (Molecular Devices, LLC, San Jose, CA), for assay validation, not required for protocol.
- Bio-Rad CFX-400 optical thermal cycler, for validation of new assays, not needed for protocol.

Infectious DWV cDNA clones tagged with green fluorescent protein and nanoluciferase reporter genes

1. The GFP-expressing DWV was generated using infectious cDNA plasmid clone DWV-L-GFP, GenBank accession number MW748704 (Ryabov et al 2020).
2. The nLuc-expression DWV, GenBank accession number MW748703, was constructed by replacing the GFP-*coding Asc*I-*BamH*I fragment of the cDNA plasmid DWV-L-GFP with the synthetic DNA sequence coding for nLuc flanked by *Asc*I and *Bam*HI restriction sites using standard molecular cloning techniques.

Production of the tagged virus inocula

3. Produce the full-length DWV-GFP or DWV-nLuc *in vitro* RNA transcripts from linearized plasmid DNA template by HiScribe T7 RNA polymerase (New England Biolabs) according to manufacturer's guidance, remove plasmid DNA template by treating with Turbo DNAse (Ambion), subsequently subject to phenol-chloroform, chloroform extraction, precipitate RNA by mixing with 2.5 volumes of ethanol and 0.1 volume of 3 M sodium acetate pH 5.2, and precipitating at 12.000 g for 15 min using microcentrifuge, wash visible pellet with 80% ethanol, air-dry, dissolve in RNAse-free water, quantify concentration using Nanodrop and store in -80^{o}C.
4. Inject white-eye honey bee pupae with 5 µg (13.2×10^{12} copies) of *in vitro* RNA transcript suspended in 8 µL of PBS.
5. Incubate pupae for 72 hours (hr) at +33^{o}C and 85% relative humidity.
6. Homogenize infected pupal tissue in 1 mL of PBS
7. Subject to three rounds of freeze-thawing and filter through a 0.22 µm nylon filter. Typically, 1 mL of the filtered extract prepared from a single transcript-injected pupae will contain 10^{9} to 10^{10} viral genome equivalents (GE), sufficient for 1000 to 10,000 pupal injections.

   Note. Filtered DWV-GFP and DWV-nLuc inocula could be produced in an equipped molecular laboratory, stored at -80^{o}C for at least 7 months and then shipped in dry ice to end users.

Injection and incubation of honey bees

8. Collect frames of sealed honey bee worker brood from colonies with low levels of the mite *Varroa destructor*, vector for DWV.
9. Harvest early stage (white-eyed or pale pink-eyed) pupae from comb brood cells, remove carefully to avoid damage, make sure that selected pupae are not *Varroa*-infested.
10. Incubate collected pupae on Whatman paper (Supplemental Figure 1A). in Petri dishes for 3 hr +33ºC and 85% relative humidity to detect and dispose pupae damaged during extraction showing development of melanization.
11. Prepare working solutions containing viral inoculum in PBS (generally 1.2×10^5 or $1.2 \times$ 107 GE of cloned DWV-GFP or DWV-nLuc per µl in for the current trials.
12. For drug testing, dissolve candidates into inocula (generally in a final solution from 1 to 10 ppm) immediately prior to injection.
13. Inject each pupa intra-abdominally, dorsal-laterally (Supplementary Fig. 1B) with 8 µl of viral inocula (with or without drugs) or PBS control using disposable insulin syringe with 31G needle, the same syringe load (typically 240 µL) could be used to inject up to 30 bees.
14. Incubate pupae at +33ºC and 85% relative humidity (Fig. 1B).

GFP fluorescence measurements for living bees

15. Acquire digital image of pupae at 0, 12, 24, 36, and 44 hours post injection (hpi) using a standard ultraviolet light table (365 nm wavelength). Each image should include PBS-injected control pupae and/or an adjacent fluorescent standard to normalize images taken on different dates with a handheld smartphone digital camera. Each image should include PBS-injected control pupae and/or an adjacent fluorescent standard to normalize images taken on different dates.

16. For UV gel imaging transilluminator (365 nm excitation) and camera use "SYBR-green" option adjust exposure time and contrast to minimize non-specific background fluorescence in the control PBS-injected pupae (Fig. 3B).

Note: 365 nm and 395 nm UV light sources are used in inexpensive and widely commercially available as "UV counterfeit currency detectors".

17. Analyze images using ImageJ (https://imagej.nih.gov) (Schneider, Rasband, & Eliceiri, 2012) for average and maximum green fluorescence of each of five pupae in each treatment group at each time point.

GFP fluorescence measurements using a 96-well fluorescence plate reader

18. Inject honey bee individuals with the GFP-tagged virus (10^4 to 10^7 genome copies) and incubate for 44 hours.
19. Homogenize the pupa with 300 µL of PBS supplemented with a protease inhibitor cocktail (cOmplete, Roche) in 1.5 mL Eppendorf tube on ice. Subject to one cycle of freeze-thaw, spin in a table-top micro centrifuge, 5,000 per minutes for 5 minutes. Collect 100 □L of supernatant for fluorimetry, freeze the rest at –80ºC for RNA extraction using TRIzol for subsequent quantification of DWV-GFP loads by RT-qPCR (Ryabov et al., 2017).
20. Autofluorescence of pupal tissue by long-wavelength UV light presents the main challenge for visualization of fluorescence of GFP, which was expressed from the viral genome in honey bee tissues. To optimize sensitivity and specificity of the GFP fluorescence detection in honeybee pupal extracts, contrast control and infected bees along a continuum of

emission wavelengths (490 nm to 600 nm) after establishing ideal excitation wavelengths (blanketed by 360 nm to 510 nm). This analysis showed that for overt levels of DWV infection, 10^{10} to 10^{12} GE per insect, optimal excitation and emission wavelengths are 480 nm and 520 nm respectively (Fig. 2B). Importantly, this analysis showed that it was possible to use non-optimal excitation UV wavelengths, 365 nm and 395 nm, which are readily available in UV transilluminators (Fig. 2B, pointed with arrows).

21. Measure emittance at optimal conditions (520 nm emission after excitation at 480 nm for the stages we tested).
22. Analyze differential emittance for GFP-carrying bees from various genetic lineages or treatments versus control samples.

nLuc activity measurements using a 96-well luminescence plate reader

23. Inject honey bee individuals with the nLuc-tagged virus, 10^5 to 10^7 genome copies and incubate for 44-48 hours. Optional: For preliminary analysis of nLuc accumulation, dissected pupae can be placed in 100 ul of NanoGlo (Promega) substrate. Bees infected with DWV-nLuc will show blue luminescence that is clearly visible by the naked eye in the dark (Fig. 4 C).
24. Homogenize the pupa with 250 µL of PBS in a 1.5 mL Eppendorf tube on ice. Subject to one cycle of freeze-thaw. Collect 1 uL (1/400th) of the bee suspension and immediately transfer it to 50 mL of 1x PBS to 200 uL wells of black, clear-bottom 96-well plates (Corning) and mix by pipetting. Freeze the rest at –80^{o}C for RNA extraction using TRIzol for subsequent quantification of DWV-GFP loads by RT-qPCR (Ryabov et al., 2017).

25. For luminescence measurements, add 50 µL of NanoGlo substrate (Promega, Cat. No. N1110), prepared according to manufacturer's instructions, to the wells of the plate containing 50 µl of an insect tissue suspension. Gently shake the plate to mix substrate and the tissue suspension and measure luminescence at 460 nm after 3 to 5 minutes, 100 ms per well. Luminescence remains constant for 10 to 15 minutes but later declines as the substrate concentration decreases.

Validation and refinement using quantitative RT-PCR

26. After measuring fluorescence, extract total RNA from samples using the TriZOL method.
27. Measure viral loads using qPCR and validated primers for DWV genome and *GFP* (Ryabov et al., 2020) or *nLuc* target sequences.
28. Use PCR thresholds (Ct values) for a dilution series of pDWV-GFP or pDWV-nLuc plasmids from 10^2 to 10^8 copies per reaction to establish an efficiency curve for the quantitative PCR runs (in our trials for DWV-GFP $\log_{10}$ GE = -0.2666 × Ct + 10.829, R^2 = 0.9889; for DWV-nLuc $\log_{10}$ GE=-0.2747 × Ct + 11.176, R^2 = 0.9978).
29. Directly quantify DWV genome copies in the samples and compare log-transformed qPCR values and estimated fluorescence using regression and ANOVA.

Troubleshooting and critical points

When choosing pupae for injection (Steps 3, 7), use honey bee colonies with low Varroa mite infestation, which are likely to have low levels of Varroa mite vectored wild type DWV. For precise single-virus studies is advisable to monitor colonies for the presence of other honey bee viruses common for the region. Each newly prepared batch of filtered DWV-GFP inoculum (Step 6) should be analysed by RT-qPCR to determine copy numbers of GFP and DWV RNA. Choose

the filtered extracts with 1:1 ratios of GFP to DWV copy numbers which has minimal proportion of the clone-derived virus with deletion of GFP. When using DWV-GFP inoculum produced by an external provider, make sure that it was delivered frozen, keep at -80^{o}C or use immediately, keep the inocula on ice. Avoid freeze thawing more than three times.

Time required

One skilled technician can inject approximately 120 bees/hour and prep the same number of bees for photographic capture in 30 minutes, followed by two hours of statistical analyses using ImageJ (Schneider et al., 2012). Injecting pupae can also be carried out via manual syringe or Micro-syringe injection pump. To quantify viral loads by fluorimetry post-experiment requires approximately four hours for 120 bees, from pulverizing bees to refinement and capture using the fluorimeter.

RESULTS

Average fluorescence of bees injected with GFP-tagged DWV or the PBS control placed on the UV transilluminator, excitation wavelengths 395 nm (Fig. 1B, 2A) or 365 nm (Figure 3A,B), was recorded using images taken with an unaided smartphone camera (Fig. 1B, 2A, 3A) or by UV gel imager camera, SYBR green set up (Fig. 3B). Filtration post-hoc using ImageJ greatly reduced autofluorescence. Fluorescence was significantly higher in infected bees versus those injected with the PBS control starting from 24 hpi, and continued to increase at 36 and 44 hpi (Fig. 1B,E, Fig. 3D), as was the estimated viral titer using qPCR (Fig. 1C,D, Fig. 3E). Note that although background levels of wild-type DWV were present even in the PBS-injected bees at low of 10^6 to 10^7 GE (Fig. 1C, PBS), only the injected DWV-GFP replicated to high levels (Fig. 1 C, D), which

was in agreement with the results of previously reported clone-derived DWV injection experiments (Ryabov et al., 2019). The use of DWV-GFP-specific pair of qPCR primers (Fig. 1A) allowed to detect exclusively the injected clone-derived virus (Fig. 1D).

Honeybee pupae infected with the novel nLuc-tagged viral construct (Fig. 4A) showed accumulation of high levels of nLuc as evidenced by strong blue luminescence (peaked at 450-460 nm) following addition of the nLuc substrate (Fig. 4 B, C). Infectivity of the filtered DWV-nLuc extract indicated that insertion of the nLuc sequence at the interface between the LP and structural genes in DWV genome did not interfere with encapsidation of viral RNA. Replication dynamics of DWV-nLuc in the pupae injected with 10^7 GE of the inoculum was similar to that of DWV and DWV-GFP (Fig. 4 D, E). Similar levels of DWV and nLuc targets determined by qRT-PCR after 48 hr post injection suggested that the nLuc insertion in DWV genome was genetically stable. The luminescent signal reached levels of 10^6 to 10^7 counts in 100 milliseconds in pupae which had 10^{10} to 10^{11} GE of DWV-nLuc (Fig. 4 F, G). Although destructive sampling (homogenisation with PBS) was required to assess the levels of accumulation of the nLuc reporter in honey bee pupae, this method showed extremely high sensitivity and a dynamic range which were both similar to those of qRT-PCR. There was practically no background in the nLuc enzymatic luminescent assay (Fig. 4C, G), and this assay is preferable when destructive sampling is possible.

Quantitative RT-PCR estimates of DWV (Fig. 1C) and DWV-GFP (Fig. 1D) were strongly correlated with both GFP fluorescence estimates (Fig. 1F; $R^2 = 0.617$) and nLuc luminescence (Fig. 4 F) was even higher than in the case of GFP reporter (Fig. 4G, $R^2 = 0.9602$). As expected, a linear dependence was observed between the log-transformed viral copy numbers quantified by qRT-PCR and log-transformed GFP fluorescence and nLuc luminescence (Fig. 1F, Fig. 4G). With a fluorometric plate reader, it was possible to refine further the optimal excitation and emissions

296 wavelengths for this assay (Fig. 2). Ultimately conditions were established with virtually no
297 masking or autofluorescence by host bee tissues, even for a range of bee life stages.
298
299 **DISCUSSION**
300 The described methods have general usefulness for tracking insect-virus dynamics. From
301 mosquitoes and other vectors of medical and veterinary importance to crop pests and beneficial
302 insects such as pollinators, being able to track viral loads in real time offers a method for resolving
303 how and when viruses proliferate in their hosts. This can predict vectoring ability and better define
304 the stages of viral infection that impact host behavior. In honey bees, these protocols provide a
305 critical tool for high-throughput screening of potential antiviral or host-enhancing drugs (Tauber
306 et al., 2019), and a further refinement of efforts to use functional genetics to better understand
307 bee/virus interactions (Gusachenko et al., 2020; Ryabov et al., 2020). This nonlethal method also
308 has considerable promise for bee breeding, since labelled individuals, once affirmed as being
309 resistant to virus infection, can be used directly in breeding efforts. Finally, the impacts of insect
310 viruses on host development and behavior are poorly understood. A system for tracking viral
311 spread and abundance in live insects should prove useful for determining more precisely when
312 infection becomes pathology.
313 These non-lethal techniques will be especially compelling for species where there is an
314 interest in heritability of immunity and disease resistance or tolerance. This interest is especially
315 high for the billion-dollar honey bee industry, but is important for evolutionary or ecological
316 studies in a diverse range of insects. As an additional benefit for non-lethal analyses of breeding
317 in Hymenoptera (ants, bees, and wasps), males in this insect order are haploid and effectively all
318 cells in their bodies, including sperm, are genetically identical. Therefore, screens for the abilities

of male hymenopterans to resist diseases provide an especially potent method for shaping breeding populations and heritability studies, since male phenotypes are traceable to single alleles. Haploid males have been exploited to identify honey bee resistance traits against parasitic mites (Conlon et al., 2019) but their power in identifying resistance to pathogens has yet to be tapped. Instrumental insemination (II) is used routinely to produce high-value breeder queens in honey bees, and II has been used for evolutionary-genetic screens in ants and wasps. This method, coupled with the 'Beeporter' scheme described here, will help address a diversity of questions related to disease genetics in social insects (Evans & Spivak, 2010).

ACKNOWLEDGEMENTS

This work was supported by the USDA - Agricultural Research Service, ARS project number 0500-00093-001-00-D, USDA National Institute of Food and Agriculture grant 2017-06481 and USDA-APHIS Interagency Agreement 18-8130-0787-IA.

COMPETING INTEREST STATEMENT

The authors declare that they have no competing interests.

AUTHOR CONTRIBUTIONS

JDE and EVR designed research, EVR designed and constructed the infectious viral constructs, EVR, OB and EP-Y performed research, all authors analysed data and wrote the paper.

DATA ACCESSIBILITY STATEMENT

342 The full-length clone of Deformed wing virus used in these trials is deposited in Genbank under
343 accession number MG831200.
344
345 **REFERENCES**
346

Figure Legends

Figure 1. A) Schematic diagram of the DWV-GFP construct (10.8 kb) and the positions of the RT-qPCR primers: "DWV" - generic DWV primers, "DWV-GFP" – tag-specific primers, and B) Successive images of bees from time of injection then 12, 24, 36, and 44 hours later, 395 nm excitation with and without filtering for autofluorescence. For each time panel, left five bees are PBS-injected control, right five – injected with 10^6 GE of DWV-GFP. C) Quantified viral loads using generic DWV primers. D) Quantified DWV-GFP virus using tag-specific primers. E) Quantified GFP fluorescence over time. F) Log_{10} transformed DWV-GFP loads (RTqPCR quantification) versus GFP fluorescence (log_{10} transformed), with best-fit regression.

Figure 2. A) Visible, original ultraviolet (365 nm excitation), and filtered ultraviolet images of bees used to test fluorimetry assay. The DWV-GFP infected bees (44 hpi) contained 7.2 x 10^{10} to 9.2 x 10^{10} genome equivalents of DWV-GFP. B) Range of excitation and emissions values (average) used to pinpoint the most accurate and sensitive conditions for the assay. Arrows indicate excitation wavelengths used in UV transilluminators (365 nm and 395 nm), and the optimal excitation wavelength (480 nm).

Figure 3. Typical simultaneous visualization of DWV infection in 120 bees, 48 hours post injection (hpi) using standard 365 nm UV transilluminator. Top left 12 bees are injected with PBS control, the rest were injected with 10^6 copies of DWV-GFP. A. Unprocessed mobile phone camera image. B. Processed gel recording camera, SYBR-green recording option. C. Visible light photograph of a subset of bees (marked in B and C), mobile phone camera image. D-F. Analysis

of the PBS and DWV-GFP-injected bees in the marked areas of A and B. D. GFP fluorescence quantified using image B, E, quantification of DWV by RT-qPCR, GE per bee, DWV-specific primers; F, estimation of honey bee actin mRNA loads, Ct values.

Figure 4. Evaluation of cDNA clone-derived DWV expression nanoluciferase (nLuc). A) Schematic diagram of the DWV-nLuc construct (10.6 kb) and the positions of the RT-qPCR primers: "DWV" - generic DWV primers, "DWV-nLuc" – tag-specific primers. B) Images of the dissected pupae 48 hours after being injected with unmodified DWV and DWV-nLuc following addition of 100mL of NanoGlo nanoluciferase substrate. The virus loads determined by RT-qPCR are shown on the left. Images of the same dissected pupae taken (left to right) with full illumination, low light and complete darkness. Blue light emission is clearly visible by the naked eye in the case of DWV-nLuc infected pupae. C). Emission spectra of the extracts of the DWV- and DWV-nLuc-infected pupae. D) Quantified viral loads using generic DWV primers. E) Quantified DWV-nLuc virus using tag-specific primers. E) Quantified nLuc activity over time. Red letters above bars indicate significantly and non-significantly different groups (ANOVA), nd – not detectable levels. F) Log10 transformed DWV-GFP loads (RTqPCR quantification) versus nLuc activity (log10 transformed luminescence intensity), with best-fit regression.

SUPPLEMENTAL DATA

Supplement Figure 1. Simultaneous visualization of DWV infection, 48 hours post injection (hpi) in 120 bees using standard 365 nm UV transilluminator, top left 12 bees are injected with PBS control. A. Bees illuminated with 365 nm UV light, unprocessed mobile phone camera image. B.

Bees illuminated with 365 nm UV light, processed gel recording camera, SYBR-green recording option. C. Visible light photograph of a subset of bees (marked in B and C), mobile phone camera image. D-F. Analysis of the PBS and DWV-GFP-injected bees in the marked areas of A and B: D - GFP fluorescence quantified using image B; E – quantification of DWV by RT-qPCR, GE per bee, DWV-specific primers; F – estimation of honeybee actin mRNA loads, Ct values.

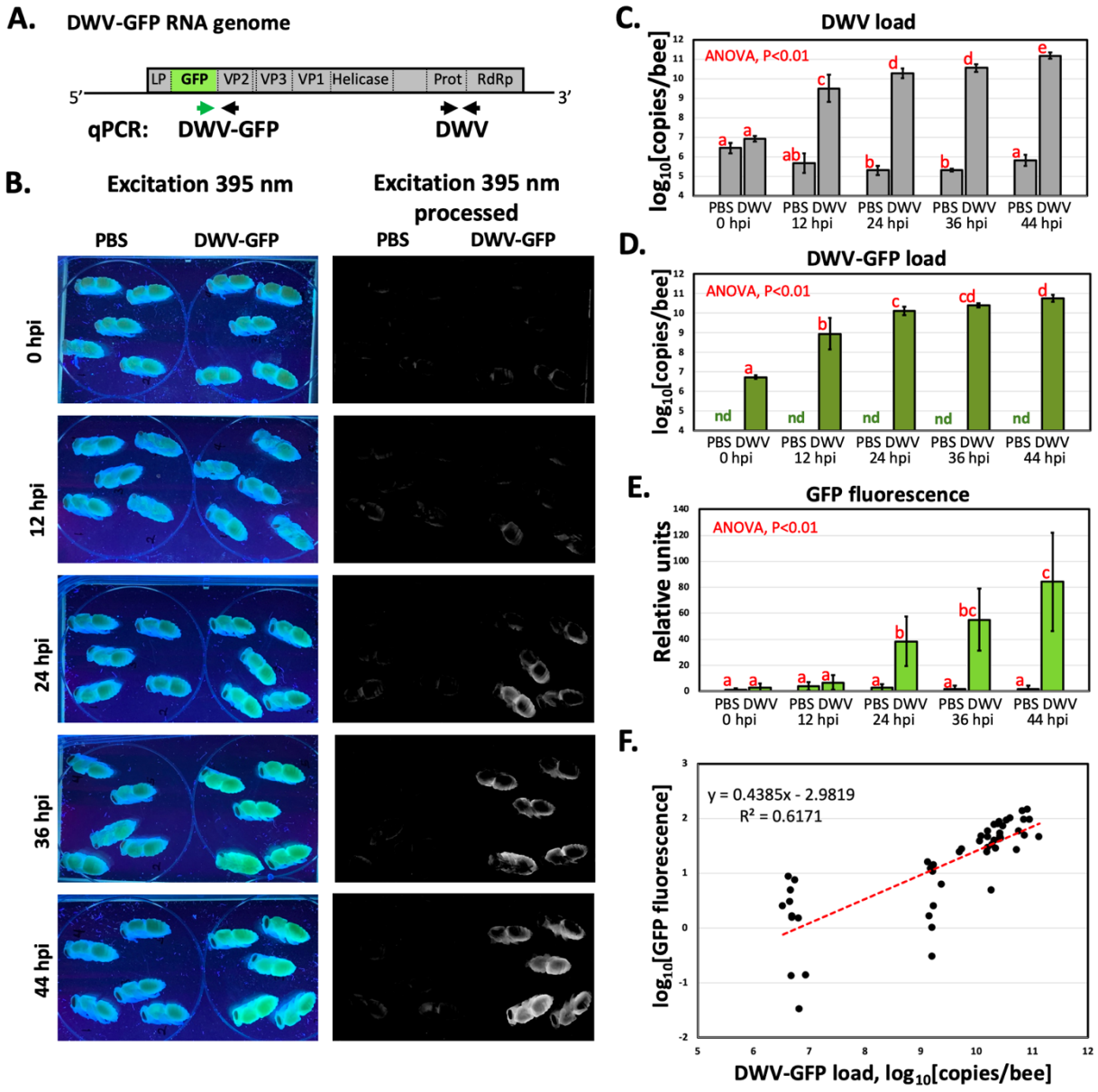
A.
DWV-GFP RNA genome
LP
GFP
VP2
VP3
VP1
Helicase
Prot
RdRp
5′
3′
qPCR:
DWV-GFP
DWV
B.
Excitation 395 nm
Excitation 395 nm processed
PBS
DWV-GFP
0 hpi
12 hpi
24 hpi
36 hpi
44 hpi
C.
DWV load
ANOVA, P<0.01
log10[copies/bee]
PBS DWV 0 hpi
PBS DWV 12 hpi
PBS DWV 24 hpi
PBS DWV 36 hpi
PBS DWV 44 hpi
D.
DWV-GFP load
ANOVA, P<0.01
log10[copies/bee]
nd
E.
GFP fluorescence
ANOVA, P<0.01
Relative units
F.
y = 0.4385x - 2.9819
R² = 0.6171
log10[GFP fluorescence]
DWV-GFP load, log10[copies/bee]

Figure 1

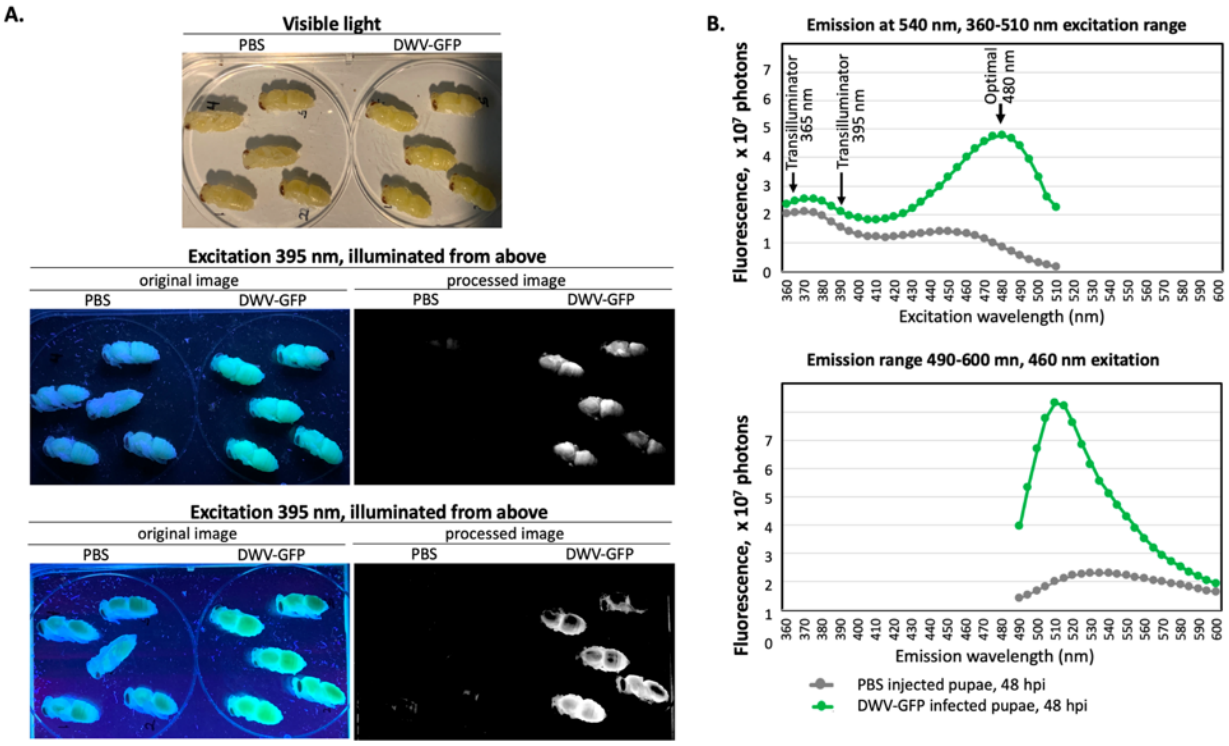
A.
Visible light
PBS
DWV-GFP
Excitation 395 nm, illuminated from above
original image
processed image
PBS
DWV-GFP
PBS
DWV-GFP
Excitation 395 nm, illuminated from above
original image
processed image
PBS
DWV-GFP
PBS
DWV-GFP
B.
Emission at 540 nm, 360-510 nm excitation range
Fluorescence, x 10⁷ photons
Transilluminator 365 nm
Transilluminator 395 nm
Optimal 480 nm
Excitation wavelength (nm)
Emission range 490-600 mn, 460 nm exitation
Fluorescence, x 10⁷ photons
Emission wavelength (nm)
PBS injected pupae, 48 hpi
DWV-GFP infected pupae, 48 hpi

Figure 2

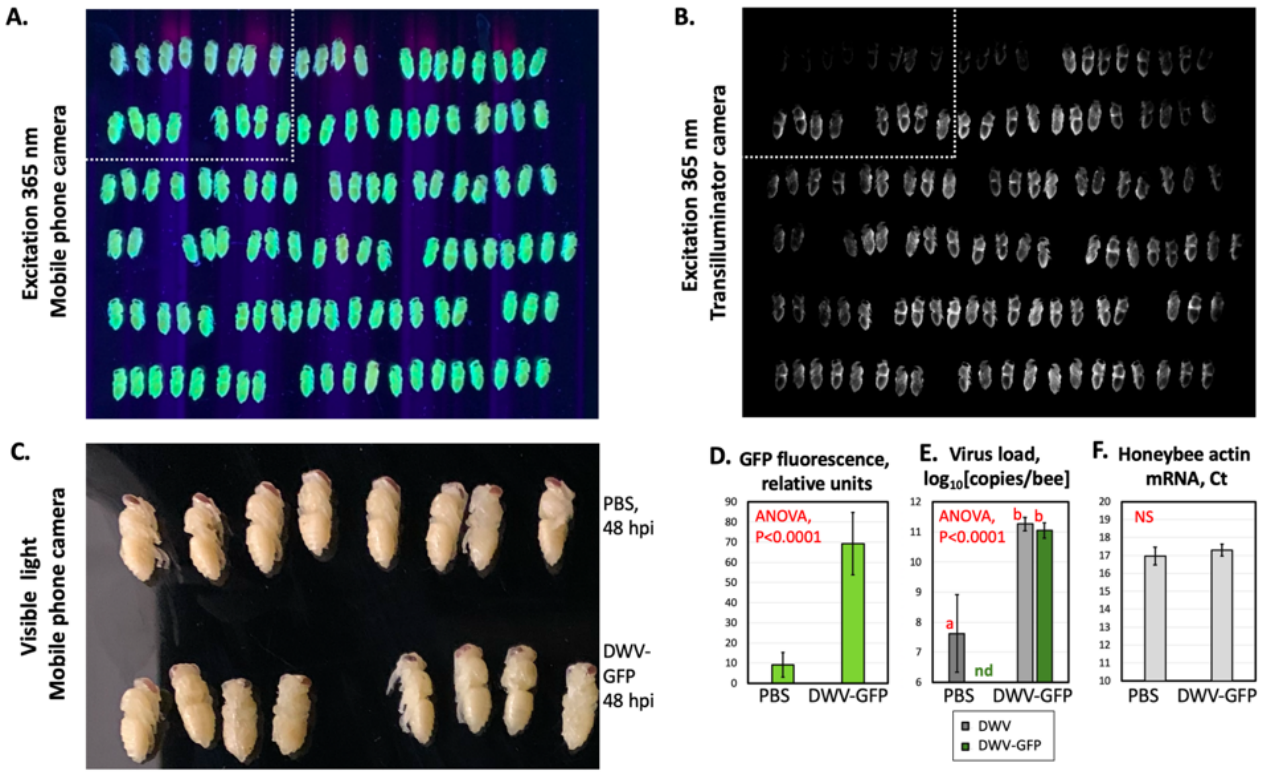
A.
Excitation 365 nm
Mobile phone camera
B.
Excitation 365 nm
Transilluminator camera
C.
Visible light
Mobile phone camera
PBS,
48 hpi
DWV-
GFP
48 hpi
D. GFP fluorescence,
relative units
ANOVA,
P<0.0001
PBS
DWV-GFP
E. Virus load,
log10[copies/bee]
ANOVA,
P<0.0001
a
b
b
nd
PBS
DWV-GFP
DWV
DWV-GFP
F. Honeybee actin
mRNA, Ct
NS
PBS
DWV-GFP

Figure 3

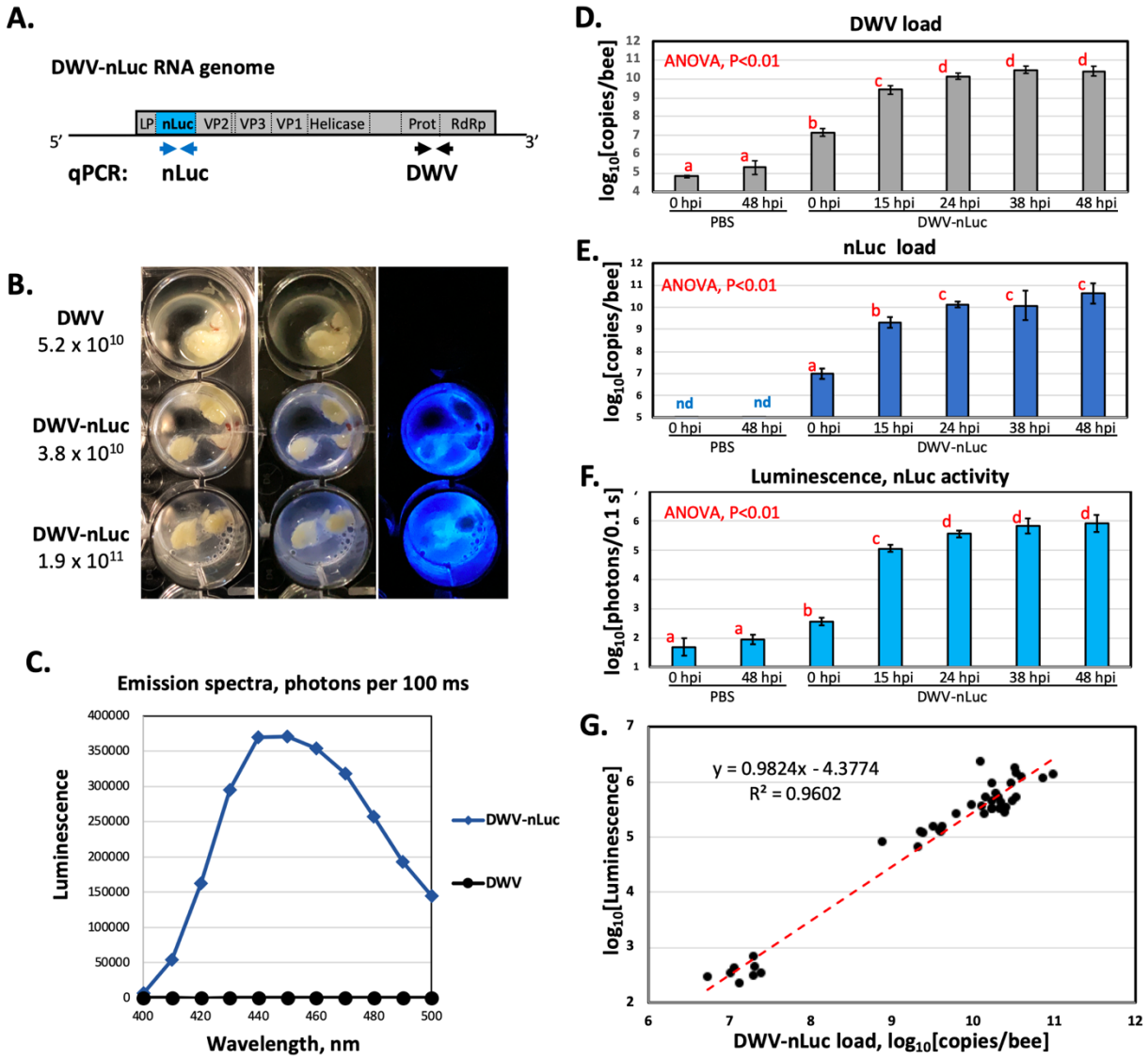

429

430 Figure 4

431

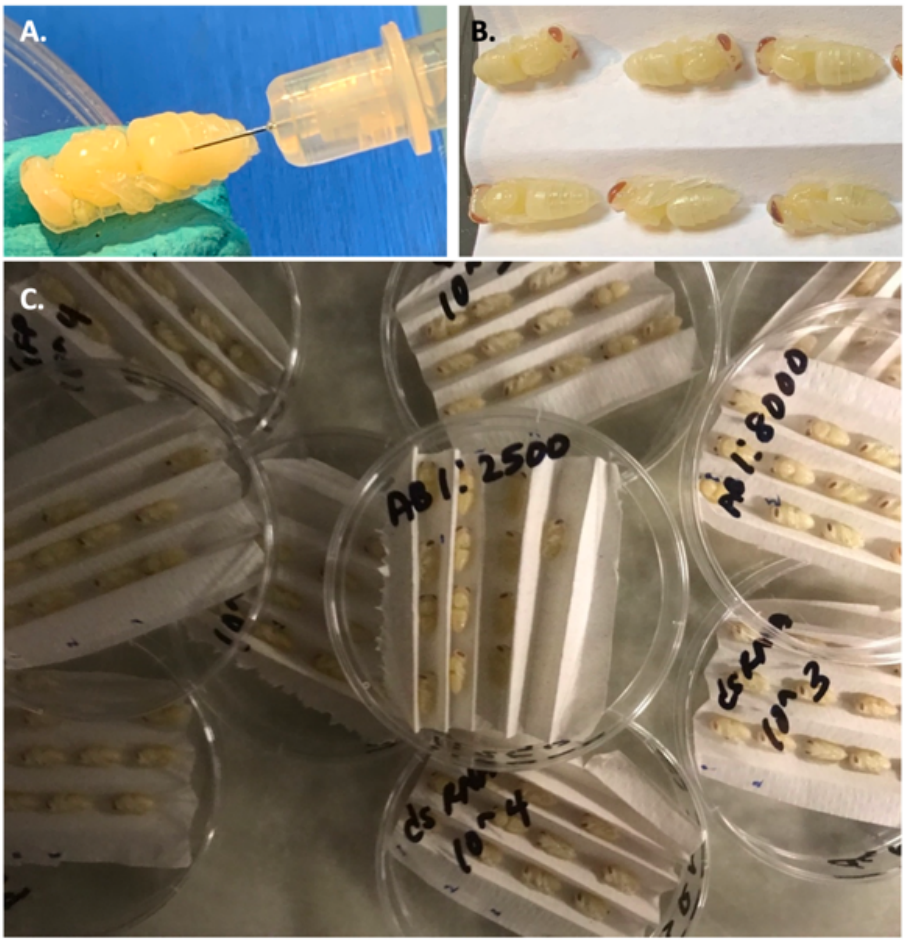

Supplemental Figure 1.

Cheng, D. J., Tian, Y. P., Geng, C., Guo, Y., Jia, M. A., & Li, X. D. (2020). Development and application of a full-length infectious clone of potato virus Y isolate belonging to SYR-I strain. *Virus Research, 276*. doi:10.1016/j.virusres.2019.197827

Chopra, S. S., Bakshi, B. R., & Khanna, V. (2015). Economic dependence of U.S. industrial sectors on animal-mediated pollination service. *Environmental Science and Technology, 49*(24), 14441-14451. doi:10.1021/acs.est.5b03788

Conlon, B. H., Aurori, A., Giurgiu, A. I., Kefuss, J., Dezmirean, D. S., Moritz, R. F. A., & Routtu, J. (2019). A gene for resistance to the Varroa mite (Acari) in honey bee (Apis mellifera) pupae. *Molecular Ecology, 28*(12), 2958-2966. doi:10.1111/mec.15080

Dainat, B., Evans, J. D., Chen, Y. P., Gauthier, L., & Neumann, P. (2012). Dead or alive: Deformed wing virus and varroa destructor reduce the life span of winter honeybees. *Applied and Environmental Microbiology, 78*(4), 981-987.

Evans, J. D., & Spivak, M. (2010). Socialized medicine: Individual and communal disease barriers in honey bees. *Journal of Invertebrate Pathology, 103*(SUPPL. 1), S62-S72.

Gallai, N., Salles, J. M., Settele, J., & Vaissière, B. E. (2009). Economic valuation of the vulnerability of world agriculture confronted with pollinator decline. *Ecological Economics, 68*(3), 810-821. doi:10.1016/j.ecolecon.2008.06.014

Grozinger, C. M., & Flenniken, M. L. (2019) Bee viruses: Ecology, pathogenicity, and impacts. In*: Vol. 64. Annual Review of Entomology* (pp. 205-226).

Gusachenko, O. N., Woodford, L., Balbirnie-Cumming, K., Campbell, E. M., Christie, C. R., Bowman, A. S., & Evans, D. J. (2020). Green bees: Reverse genetic analysis of deformed wing virus transmission, replication, and tropism. *Viruses, 12*(5). doi:10.3390/v12050532

Hall, M. P., Unch, J., Binkowski, B. F., Valley, M. P., Butler, B. L., Wood, M. G., . . . Wood, K. V. (2012). Engineered luciferase reporter from a deep sea shrimp utilizing a novel imidazopyrazinone substrate. *ACS Chemical Biology, 7*(11), 1848-1857. doi:10.1021/cb3002478

Mei, Y., Liu, G., Zhang, C., Hill, J. H., & Whitham, S. A. (2019). A sugarcane mosaic virus vector for gene expression in maize. *Plant Direct, 3*(8). doi:10.1002/pld3.158

Nazzi, F., & Pennacchio, F. (2018). Honey bee antiviral immune barriers as affected by multiple stress factors: A novel paradigm to interpret colony health decline and collapse. *Viruses, 10*(4). doi:10.3390/v10040159

Rollin, O., Vray, S., Dendoncker, N., Michez, D., Dufrêne, M., & Rasmont, P. (2020). Drastic shifts in the Belgian bumblebee community over the last century. *Biodiversity and Conservation, 29*(8), 2553-2573. doi:10.1007/s10531-020-01988-6

Rosenberger, D. W., & Conforti, M. L. (2020). Native and agricultural grassland use by stable and declining bumble bees in Midwestern North America. *Insect Conservation and Diversity, 13*(6), 585-594. doi:10.1111/icad.12448

Ryabov, E. V., Childers, A. K., Chen, Y., Madella, S., Nessa, A., VanEngelsdorp, D., & Evans, J. D. (2017). Recent spread of Varroa destructor virus-1, a honey bee pathogen, in the United States. *Scientific Reports, 7*(1). doi:10.1038/s41598-017-17802-3

Ryabov, E. V., Childers, A. K., Lopez, D., Grubbs, K., Posada-Florez, F., Weaver, D., . . . Evans, J. D. (2019). Dynamic evolution in the key honey bee pathogen deformed wing virus: Novel insights into virulence and competition using reverse genetics. *PLoS Biology, 17*(10). doi:10.1371/journal.pbio.3000502

Ryabov, E. V., Christmon, K., Heerman, M. C., Posada-Florez, F., Harrison, R. L., Chen, Y., & Evans, J. D. (2020). Development of a honey bee RNA virus vector based on the genome of a deformed wing virus. *Viruses, 12*(4). doi:10.3390/v12040374

Schneider, C., Rasband, W., & Eliceiri, K. (2012). NIH Image to ImageJ: 25 years of image analysis. *Nature Methods, 9*(7), 671-675.

Steinhauer, N., Kulhanek, K., Antúnez, K., Human, H., Chantawannakul, P., Chauzat, M. P., & vanEngelsdorp, D. (2018). Drivers of colony losses. *Current Opinion in Insect Science, 26*, 142-148. doi:10.1016/j.cois.2018.02.004

Tauber, J. P., Collins, W. R., Schwarz, R. S., Chen, Y., Grubbs, K., Huang, Q., . . . Evans, J. D. (2019). Natural product medicines for honey bees: Perspective and protocols. *Insects, 10*(10). doi:10.3390/insects10100356

Tehel, A., Streicher, T., Tragust, S., & Paxton, R. J. (2020). Experimental infection of bumblebees with honeybee-associated viruses: No direct fitness costs but potential future threats to novel wild bee hosts: Experimental infection of B. terrestris. *Royal Society Open Science, 7*(7). doi:10.1098/rsos.200480rsos200480

Wang, Y., He, W., Li, Q., Xie, X., Qin, N., Wang, H., . . . Wei, Z. (2020). Generation of a porcine reproductive and respiratory syndrome virus expressing a marker gene inserted between ORF4 and ORF5a. *Archives of Virology, 165*(8), 1803-1813. doi:10.1007/s00705-020-04679-3

Xie, X., Muruato, A. E., Zhang, X., Lokugamage, K. G., Fontes-Garfias, C. R., Zou, J., . . . Shi, P.-Y. (2020). A nanoluciferase SARS-CoV-2 for rapid neutralization testing and screening of anti-infective drugs for COVID-19. *Nature Communications, 11*(1), 5214. doi:10.1038/s41467-020-19055-7